ELSEVIER

Polymer 44 (2003) 2547–2551

polymer

www.elsevier.com/locate/polymer

Kinetics of non-isothermal cold crystallization of uniaxially oriented poly(ethylene terephthalate)

Z. Zhang*, M. Ren, J. Zhao, S. Wu, H. Sun

School of Materials Science and Chemical Engineering, Tianjin Polytechnic University, 300160 Tianjin, People's Republic of China

Received 9 September 2002; received in revised form 17 December 2002; accepted 15 January 2003

Abstract

The non-isothermal equation was extended to describe non-isothermal cold crystallization kinetics of oriented polymers. The validity of the equation was examined by using a DSC crystallization curve of oriented poly(ethylene terephthalate) (PET) fibers with a constant heating rate. The double cold crystallization peaks appeared in the DSC curve. The relative degrees of crystallinity at different temperatures were analyzed by using the equation. The results show that the value of the Avrami exponent near to 1 at lower temperatures implies the bundle-like crystal growth geometry and the value of the Avrami exponent near to, 2, at higher temperatures implies the higher dimension crystal growth geometry. The first crystallization process crystallizes at faster rate than that of the isotropic sample, while the second process crystallizes at slower rate than that of isotropic sample. If a simple single process model was used, the value of the Avrami exponent, 0.77, was obtained. The result shows the simple single process model cannot describe the processes of crystallization of oriented PET fibers satisfactorily.

Keywords: Non-isothermal crystallization; Orientation; Poly(ethylene terephthalate)

1. Introduction

Non-isothermal crystallization theory and methods possess practical importance both in the simulation of technological processes and in the determination of parameters of crystallization kinetics of crystallizable polymers. In order to determine parameters of crystallization kinetics of polymers, a few equations and methods were proposed. Ozawa [1] derived a non-isothermal kinetics equation from the basic Evans theory by considering the process of nucleation and its growth. From the Ozawa equation, the Avrami exponent and the cooling function for non-isothermal crystallization at given temperatures can be obtained by using DSC curves with several constant cooling or heating rates. Harnisch and Muschik [2] derived an equation based on the Avrami theory, which can obtain the Avrami exponent by using DSC curves with two constant cooling rates. Jeziorny [3] and Privalko [4] also extended the Avrami equation to non-isothermal crystallization situations. They treated the DSC curve of non-isothermal crystallization as the isothermal one, calculated the parameters of crystallization rate constant and the Avrami exponent, and then corrected the corresponding parameters. Mo and co-workers [5] proposed another non-isothermal equation by combining the Ozawa and the Avrami equations, from which the ratio of the Avrami exponent to the Ozawa exponent and another parameter can be obtained. Dutta [6] presented an equation from which the Avrami exponent and the activation energy can be gained by using several DSC heating curves. Caze et al. [7] extended the Ozawa equation and suggested a set of equations to obtain the Avrami exponent and the cooling function. Khanna [8] introduced a parameter called 'crystallization rate coefficient' (CRC) measured from the slope of the plot of cooling rates versus crystallization peak temperatures. One of the present authors, Zhang [9], developed an equation and method, from which the Avrami exponent and the crystallization rate constant can be obtained, which is close to one obtained from the isothermal method crystallized at different temperatures. Up to date, the non-isothermal crystallization theory and methods have drawn some authors' attention [10–17].

* Corresponding author. Tel.: +86-22-24528463; fax: +86-22-24528054.
E-mail address: zhangz@public.tpt.tj.cn (Z. Zhang).

0032-3861/03/$ - see front matter © 2003 Elsevier Science Ltd. All rights reserved.
doi:10.1016/S0032-3861(03)00105-8

The non-isothermal crystallization models proposed previously, however, didn't take the multi-processes of crystallization into account. Experiments have shown that the double peaks, even more peaks, appeared in DSC curves of oriented PET fibers [18–19]. This meant that the multiple crystallization processes occur and the current non-isothermal crystallization models are not suitable for describing oriented polymer crystallization processes accurately. The purpose of this study is to develop a new model to describe the crystallization processes of oriented polymer and test its validity.

2. Theory

2.1. Non-isothermal crystallization model

By taking into account the situation of polymer crystallization, the Avrami theory can be expressed in following form [20,9]:

$$\frac{dV}{dV_{ex}} = 1 - \alpha \tag{1}$$

where V represents the real volume of crystalline phase per unit volume; V_{ex}, the 'extended' volume of the crystalline phase, that is, assuming that possible overlapping of growing entities is neglected; α, the relative volume degree of crystallinity. Eq. (1) is not limited to isothermal conditions, so it can be used in non-isothermal cases. Eq. (1) can be converted into

$$\frac{dV}{dt} = \frac{dV_{ex}}{dr}\frac{dr}{dt}(1 - \alpha) \tag{2}$$

where dr/dt is the increment of crystalline entities in the direction of growth within unit time. Actually, it represents the linear growth rate of the entities. Many experiments have proved that dr/dt only depends on temperature for a given polymer. By considering relationships between dV_{ex}/dr and α, the following non-isothermal equation can be derived from Eq. (2) [9]:

$$\frac{d\alpha}{dt} = K(T)[-\ln(1 - \alpha)]^m(1 - \alpha) \tag{3}$$

where $K(T)$ is the crystallization rate constant, being dependent on temperature; m is related to the mechanism of crystallization. The physical significance of $K(T)$ and m are listed in Table 1.

In the table, N_0 is the number of nuclei per unit volume; X_e, the volume degree of crystallinity at the end of crystallization; d_0, the thickness of a disk-shape entity; S', the surface area of the cross-section of a rod-like entity. k, the ratio of the nucleation rate to linear growth rate of crystalline entities; G, the linear growth rate of the entities.

Table 1
The physical significance of $K(T)$ and m in Eq. (3)

Shape	m	$K(T)$
Instantaneous nucleation		
Sphere	2/3	$4\pi N_0 G(3X_e/4\pi N_0)^{2/3}/X_e$
Disk	1/3	$2G(\pi d_0 N_o X_e)^{1/2}/X_e$
Rod	0	$N_0 S' G/X_e$
Sporadic nucleation		
Sphere	3/4	$(4/3)\pi k G(3X_e/\pi k)^{3/4}/X_e$
Disk	2/3	$\pi d_0 G k(3X_e/\pi d_0 k)^{2/3}/X_e$
Rod	1/2	$G(2X_e S' k)^{1/2}/X_e$

2.2. Models for uniaxially oriented polymer

The crystallization rate constant $K(T)$ in Eq. (3) is dependent on temperature and can be described by [21–23]

$$K(T) = K_0 \exp\left(-\frac{E_d}{RT} - \frac{\psi T_m^{0^2}}{T^2(T_m^0 - T)}\right) \tag{4}$$

where K_0 is approximate to a constant; E_d, the activation energy of diffusion of crystallizing segments across the phase boundary; ψ is referred to as the nucleation parameter related to the surface free energy of forming crystals, the melting enthalpy, etc. T_m^0, the equilibrium melting temperature; R, the gas constant. By assuming that diffusion of segments predominates over crystallization rate in the DSC heating process, Eq. (4) degenerates into [19]

$$K(T) = K_0 \exp\left(-\frac{E_d}{RT}\right) \tag{5}$$

A similar expression was also used by Cebe and Hong who assume a thermally activated process occurs [24]. Rearranging and integrating Eq. (3) and taking Eq. (5) into account, we obtain

$$\alpha = 1 - \exp\left\{-\left[\frac{K_0}{n\beta}\int_{T_0}^{T}\exp\left(-\frac{E_d}{RT}\right)dT\right]^n\right\} \tag{6}$$

where β is the heating rate ($= dT/dt$); T_0, the temperature at which the crystallization begins to occur; n, the Avrami exponent, $n = 1/(1 - m)$ [9]. By substituting following approximate expression [25]

$$\int_{T_0}^{T}\exp\left(-\frac{E_d}{RT}\right)dT \approx \frac{RT^2}{E_d}\cdot\exp\left(-\frac{E_d}{RT}\right)\cdot\left(1 - \frac{2RT}{E_d}\right) \tag{7}$$

into Eq. (6), the non-isothermal crystallization equation becomes

$$\alpha = 1 - \exp\left\{-\left[\frac{K_0}{n\beta}\cdot\frac{RT^2}{E_d}\cdot\exp\left(-\frac{E_d}{RT}\right)\cdot\left(1 - \frac{2RT}{E_d}\right)\right]^n\right\} \tag{8}$$

The appearance of the multi-peaks in the DSC curve of uniaxially oriented PET fibers means the different crystallization processes occur during the DSC scanning process.

By assuming the whole crystallization process is composed of superimposition of several single crystallization processes, the whole relative degree of crystallinity at a given time is thus given by

$$\alpha = \sum_{i}^{k} \omega_i \alpha_i \tag{9}$$

where k should be an integer, such as $1, 2, 3, \ldots$, determined by the number of peaks appearing in the DSC crystallization curve; ω_i is the weight fraction of crystals formed by the ith crystallization process, thus, $\sum_i^k \omega_i = 1$; α_i is the relative degree of crystallinity of a single process. As every process has its own mechanism and crystallization rate, α_i can be expressed as

$$\alpha_i = 1 - \exp\left\{-\left[\frac{K_{0i}}{n_i \beta} \cdot \frac{RT^2}{E_{\mathrm{d}i}} \cdot \exp\left(-\frac{E_{\mathrm{d}i}}{RT}\right) \cdot \left(1 - \frac{2RT}{E_{\mathrm{d}i}}\right)\right]^{n_i}\right\} \tag{10}$$

Crystallization processes of uniaxially oriented polymers can be described by both Eqs. (9) and (10).

3. Experimental and calculation

3.1. Experiments

The PET was synthesized by using the conventional two stage method with intrinsic viscosity of 0.53 dl/g determined with an Ubbelohde viscometer in a concentration of 0.5% weight percent in o-chlorophenol at 25 °C. The non-metal catalyst was adopted. The chips were dried to make the residual water less than 2 ppm before they were injected into fibers. The polymer melt was spun at 270 °C. The winding speed was 430 m/min. The as-spun fibers were drawn on a hot metal plane at 70 °C and at a rate of 152.7 m/min. The drawn ratio was 4.023.

The transmission wide-angle X-ray diffraction experiments were performed on the sample by using a flat-film camera and a Regaku D/max-r A X-ray diffractometer, respectively, showing no obvious crystals occurred in the oriented PET fibers. The crystallization process was traced by a Perkin–Elmer DSC-7 under a nitrogen atmosphere at a heating rate of 20 °C/min. The sample weight of 5 mg was adopted.

3.2. Calculation method

The multi-peaks were resolved by using the least square method. Every single peak was described by using the Gaussian function. The weight fraction of every crystallization process, ω_i, can be calculated in terms of areas of peaks. The parameters, K_{0i}, n_i and $E_{\mathrm{d}i}$, can be obtained by using Eqs. (9) and (10) to fit the relative degree of crystallinity at different temperatures based on non-linear curve fitting method.

4. Results and discussion

4.1. Resolving overlapping peaks

The oriented non-crystalline PET fibers can crystallize at lower temperature in the DSC scanning process than the isotropic PET ones. The DSC curve was transformed into that of $\mathrm{d}\alpha/\mathrm{d}t$ versus T and then the curve was resolved by using the Gaussian function, as shown in Fig. 1. We can find the peaks can be fitted well with the Gaussian function. The area fraction of the peak at lower temperatures is 0.57; the one at higher temperatures is 0.43.

4.2. Fitting of relative degree of crystallinity

The data of relative degrees of crystallinity of oriented PET fibers at different temperatures were fitted with Eqs. (9) and (10). In order to compare it with an isotropic sample, we also carried out a fitting of the data of isotropic PET by using the single process model, Eq. (8). The parameters obtained from the fitting are listed in Table 2, from which the curves of the relative degree of crystallinity versus temperatures were calculated in terms of Eqs. (9) and (10) for oriented PET and Eq. (8) for isotropic PET, as shown in Fig. 2.

It is clearly shown that oriented PET can crystallize at lower temperatures. And the predicted curves are very consistent with the experimental data obtained from DSC crystallization curves.

4.3. Crystallization mechanism

The value of the Avrami exponent is the reflection of the crystallization mechanism. The Avrami exponent of the first crystallization process is lower than that of the second crystallization process. This shows that crystals grew in lower dimensions at lower temperatures and in higher dimensions at higher temperatures. At lower temperatures, the Avrami exponent was found to be close to 1, suggesting the bundle-like growth geometry with an instantaneous

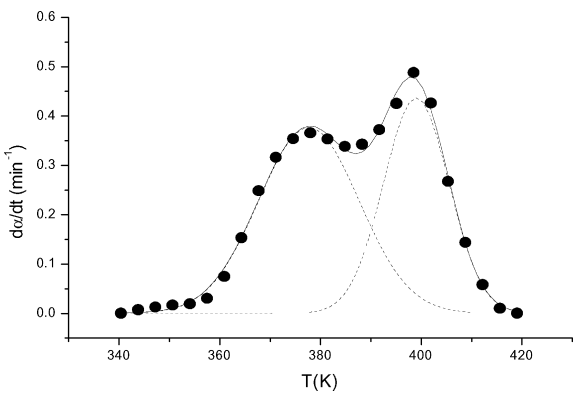

Fig. 1. The plots of $\mathrm{d}\alpha/\mathrm{d}t$ vs temperature; dots were obtained from the DSC curve; dashed lines were the resolved peaks; solid line was predicated data.

Table 2
Parameters of crystallization kinetics of PET

Samples	E_d (KJ/mol)	n	K_0 (min^{-1})
Oriented PET			
Process 1	103.69	1.04	3.12×10^{14}
Process 2	96.61	1.97	1.05×10^{13}
Isotropic PET	109.68	3.43	8.45×10^{14}

nucleation process. At higher temperatures, the value of the Avrami exponent is nearly equal to 2, suggesting the crystals formed possess higher dimensions and, perhaps, chain folded crystals were partially formed.

The Avrami exponents of oriented PET were released in some papers with some conflicting results. Generally, the changing trend of the Avrami exponent is toward a lower value with an increase in non-crystalline orientation prior to crystallization [26,27]. Some authors reported that the Avrami exponents are even less than unity [28–30]. The conflicting results reflects either the complexity of oriented PET or that the crystallization processes in an oriented PET are too fast to be followed by most of the isothermal method [31]. We found if the Avrami exponent was limited to the range from 4 to 1, the value of unity was obtained [18,19], suggesting the crystallization process can be approached by a first order rate equation under non-isothermal condition. We use the single process model, Eq. (8), and limit Avrami exponent to range from 1 to 4 to follow the crystallization process and then the same result can be obtained as the reference [19]. If the limit of the Avrami exponent is removed, we obtain the value of the Avrami exponent of 0.77, which shows the complexity of crystallization of oriented PET and the single process model cannot describe the processes of crystallization of uniaxially oriented PET satisfactorily. The value of the Avrami exponent is related not only to samples, but also to models describing crystallization processes.

The Avrami exponent of isotropic PET is located between 3 and 4, suggesting spherical growth geometry with both instantaneous and sporadic nucleation mechanisms.

4.4. Crystallization rate constant and activation energy

The crystallization rate constant was calculated according to Eq. (5) by using the parameters listed in Table 2, as shown in Fig. 3.

It can be found that, at a given temperature, crystallization rate of the first process is higher than that of isotropic PET, but the rate of the second process is lower than that of isotropic PET. The reason is that drawing results in a more ordered non-crystalline superstructure that can crystallize in a faster mode. As the temperature rises, the increase of disorientation or the decrease of the ordered part reduces the rate of crystallization and changes the crystal growth morphology, which makes crystallization rate of the second process decreases.

The activation energy, E_d, of the oriented sample are 96.61 KJ/mol for the first process and 103.69 KJ/mol for the second process. The values are somewhat lower than the 109.68 KJ/mol obtained from the isotropic sample. Some different values of E_d were given in the literature. Sun et al., reported Ed in range of 58.5–246.6 KJ/mol for different oriented samples [31]. Miller reported a value of $E_d = 184$ KJ/mol for undrawn PET filaments [32]. Okui found that Ed of PET is equal to 163.4 KJ/mol [33]. Mayhan et al., gave a value of 154.7 KJ/mol [34]. Kim and Mandelkern reported Ed in range of 80–86 KJ/mol [35]. In our previous work [23], we gave the values of E_d in the range of 86.5–125.9 KJ/mol calculated in a different method, which is in correspondence with 96.6–109.7 KJ/mol in this paper. The result indicates the E_d values obtained in current paper are also reasonable.

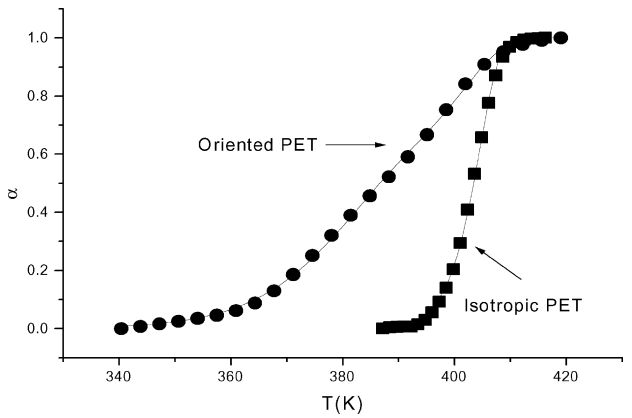

Fig. 2. The temperature dependence of relative degree of crystallinity; dots were the experimental data for oriented PET; squares were the experimental data for isotropic PET; solid lines were the predicted curves in terms of Eqs. (9) and (10) for oriented PET and Eq. (8) for isotropic PET.

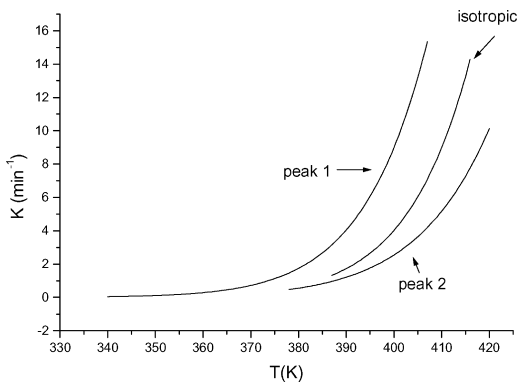

Fig. 3. The temperature dependence of the crystallization rate constant of PET fibers.

5. Conclusion

The non-isothermal equation obtained in the current paper can be used to describe the crystallization process of polymers traced by DSC at a constant heating rate. The Avrami exponent and the crystallization rate constant can be obtained by the method.

The uniaxially oriented PET crystallization curve was analyzed by using the equations. The first crystallization process corresponds to the value of the Avrami exponent close to 1, suggesting the bundle-like crystal morphology with instantaneous nucleation mechanism. The second process at higher temperatures corresponds to the value of the Avrami exponent being close to 2, implying the higher dimensions growth geometry.

Acknowledgements

The authors are grateful for financial support granted by Tianjin Municipal High Education Commission for the Developing Fund of Science and Technology (project number: 990716). We would also like to express our thanks to Mr Samuel Macdonald (H.H. Wills laboratory, the University of Bristol, UK) for his kind help during the composition of this paper.

References

[1] Ozawa T. Polymer 1971;12:150–8.
[2] Harnisch K, Muschik H. Colloid Polym Sci 1983;261:908–13.
[3] Jeziorny A. Polymer 1978;19:1142–4.
[4] Privalko VP, Kawai T, Lipatoo YuS. Colloid Polym Sci 1979;257:1042–8.
[5] Liu T, Mo Z, Zhang H. J Appl Polym Sci 1998;67:815–21.
[6] Dutta A. Polym Commun 1990;31:451–2.
[7] Caze C, Devaux E, Crespy A, Cavrot JP. Polymer 1997;38:497–502.
[8] Khanna YP. Polym Eng Sci 1990;30:1615–9.
[9] Zhang Z. Chinese J Polym Sci 1994;12:256–65.
[10] Choe CR, Lee KH. Polym Eng Sci 1989;29:801–5.
[11] Hammami A, Mehrotra AK. Polym Eng Sci 1995;35:170–2.
[12] Di Lorenzo ML, Silvestre C. Prog Polym Sci 1999;24:917–50.
[13] Mubarak Y, Harkin-Jones EMA, Martin PJ, Ahmad M. Polymer 2001;42:3171–82.
[14] Martin JA, Cruz Pinto JJC. Polymer 2000;41:6875–84.
[15] Phillips R, Manson JE. J Polym Sci, Polym Phys 1997;35:875–88.
[16] Ding Z, Spruiell JE. J Polym Sci, Polym Phys 1997;35:1077–93.
[17] Zhang Z, Zhao J. China Synthetic Fiber Industry 2000;23(1):56–8.
[18] Zhang Z. China Synthetic Fiber Industry 1997;20(5):16–19.
[19] Zhang Z, Zhao J. Acta Polymerica Sinica 1996;(3):374–7.
[20] Avrami M. J Chem Phys 1940;8:212–24.
[21] Mandelkern L, Jain NL, Kim H. J Polym Sci, Polym Phys 1968;6:165–80.
[22] Hoffman JD. J Chem Phys 1958;29:1192–3.
[23] Zhang Z, Gu G. Acta Polymerica Sinica 1992;(5):557–63.
[24] Cebe P, Hong SD. Polymer 1986;27:1183–92.
[25] Chen J, Li C. Thermal Analysis and its Application. Beijing: Academic Press; 1985. p. 267.
[26] Kiflie Z, Piccarolo S, Brucato V, Balta-Calleja FJ. Polymer 2002;43:4487–93.
[27] Althen G, Zachmann HG. Makromol Chem 1979;180:2723–33.
[28] Desai P, Abhiraman AS. J Polym Sci, Polym Phys 1985;23:653–74.
[29] Bragato G, Gianotti G. Eur Polym J 1983;19:803–9.
[30] Smith FS, Steward RD. Polymer 1974;15:283–6.
[31] Sun T, Pereira J, Porter RS. J Polym Sci, Polym Phys 1984;22:1163–71.
[32] Miller B. J Appl Polym Sci 1967;11:2343–8.
[33] Okui N. Polym Bull 1990;23:111–8.
[34] Mayhan KG, James WJ, Bosch W. J Appl Polym Sci 1965;9:3605–16.
[35] Kim H, Mandelkern L. J Polym Sci Part A-2 1968;6(4):695–706.